Bull. Chem. Soc. Jpn., 74, 1623–1628 (2001)

Synthesis, Structure, and Characterization of an α-Dawson-type $[S_2W_{18}O_{62}]^{4-}$ Complex

Sadayuki Himeno,*[*] Hideki Tatewaki, and Masato Hashimoto[†]

Department of Chemistry, Faculty of Science, Kobe University, Kobe 657-8501

†Department of Material Science and Chemistry, Faculty of System Engineering, Wakayama University,
Sakaedani, Wakayama 640-8510

(Received March 7, 2001)

A yellow sulfatotungstate complex was formed by heating a 50 mM W(VI)–2 M H_2SO_4–40% (v/v) CH_3CN system at 70 °C for 14 days, being isolated as the tetrapropylammonium (n-Pr_4N^+) salt. An X-ray structural analysis (orthorhombic, $Pca2_1$ (No. 29) $a = 27.181(1)$, $b = 14.1428(6)$, $c = 27.7292(9)$ Å, and $Z = 4$) revealed that the structure consists of an α-Dawson-type $[S_2W_{18}O_{62}]^{4-}$ anion. The α-$[S_2W_{18}O_{62}]^{4-}$ complex underwent a four-step reversible one-electron reduction in CH_3CN, and the presence of acid caused the one-electron waves to be converted into three two-electron waves. The formation conditions were elucidated by a combined Raman and voltammetric study.

The utility of heteropoly complexes has stimulated interest in the preparation of these compounds. Among heteropoly complexes, the so-called Dawson complexes have received considerable attention due to their possible use in electrocatalysis and electroanalysis; $[P_2W_{18}O_{62}]^{6-}$,[1–5] $[As_2W_{18}O_{62}]^{6-}$,[6] $[P_2Mo_{18}O_{62}]^{6-}$,[7,8] and $[As_2Mo_{18}O_{62}]^{6-}$ complexes[9] have already been prepared from aqueous solutions.

Our recent attention has been focused on the preparation of heteropoly complexes incorporating S(VI) as the central heteroatom. No molybdosulfate complexes had been known prior to our previous reports on the Dawson-type α-$[S_2Mo_{18}O_{62}]^{4-}$ complex.[10] Subsequently, we prepared and structurally characterized Strandberg-type $[S_2Mo_5O_{23}]^{4-}$ and Keggin-type α-$[SMo_{12}O_{40}]^{2-}$ complexes.[11,12] The presence of water-miscible organic solvents, such as CH_3CN and C_2H_5OH, is essential for the formation of these molybdosulfate complexes. As far as tungstosulfate complexes are concerned, the γ-Dawson-type $[S_2W_{18}O_{62}]^{4-}$ complex has recently been prepared.[13]

Continuing our preparative studies on heteropoly complexes, we now report on the synthesis of an α-Dawson-type $[S_2W_{18}O_{62}]^{4-}$ complex. Like the molybdosulfate complexes mentioned above, the α-$[S_2W_{18}O_{62}]^{4-}$ complex is formed only in the presence of CH_3CN in the W(VI)–H_2SO_4 system. The present paper describes the synthesis, structure, and characterization of the new complex.

Experimental

Instrumentation. Voltammetric measurements were performed using a Hokuto Denko HA-501 potentiostat interfaced with a microcomputer-controlled system. The working electrode was a Tokai glassy carbon rod (GC-30S) with a surface area of 0.20 cm^2. The GC electrode was polished manually with 0.25 µm diamond slurry before each measurement. A three-electrode system was employed with a platinum wire used as the counter electrode. The reference electrode was an Ag/AgCl electrode for the CH_3CN–water solution or an Ag/Ag$^+$ (0.01 M; CH_3CN) for the CH_3CN solution; the redox potentials of a ferrocene/ferricinium couple were found to be 0.27 and 0.06 V against the respective reference electrodes. The voltammetric measurements were made at 25±0.1 °C. Unless otherwise noted, the voltage scan rate was set at 100 mV/s. Raman spectra were obtained with a Jobin Yvon Ramanor U-1000 spectrophotometer equipped with a liquid nitrogen-cooled CCD detector. An argon ion laser at 488 nm was used for Raman excitation. The laser power was 50 mW at the sample. For quantitative measurements, the Raman intensities were normalized with the intensity of the 924 cm^{-1} line due to the absorption of CH_3CN in the CH_3CN–water media. A Hitachi 270-30 spectrophotometer was used to record IR spectra in the range of 1700–400 cm^{-1} in KBr pellets. TG–DTA measurements were performed with a Rigaku TAS-100 thermal analyzer. The contents of W(VI) and SO_4^{2-} were determined with a Hitachi high-performance liquid chromatograph with a Tosoh TSKgel-IC-Anion-PW_{XL} column. All other chemicals were of analytical grade and were used as received.

Synthesis. To a 16.5 g solution of $Na_2WO_4 \cdot 2H_2O$ in 490 mL of water was added 400 mL of CH_3CN. Then, 110 mL of conc. H_2SO_4 was added dropwise with vigorous stirring; suspension occurred upon the addition of a few drops of conc. H_2SO_4, and the next drops were added after the suspension had been cleared within several seconds. This procedure gave a clear pale-yellow solution of $[W_{10}O_{32}]^{4-}$. The solution was heated at 70 °C for 14 days. During this time the solution changed to yellow with the appearance of a colloidal precipitate. After the solution was cooled to room temperature, 300 mL of CH_3CN was added to produce two liquid layers. After the lower turbid layer was discarded, 10 g of n-Pr_4NBr was added to precipitate a yellow salt. The salt was collected by filtration, washed with water and ethanol, and air-dried to yield 7.5 g of the product, which was subsequently purified by recrystallization from 200 mL of CH_3CN at room temperature. Anal. Calcd for $(n\text{-}Pr_4N)_4[S_2W_{18}O_{62}]$: C, 11.28; H, 2.21; N, 1.10; S, 1.25; W, 64.8%. Found: C, 11.25; H, 2.24; N, 1.10; S, 1.25; W, 64.9%. In the TG–DTA measurement, no CH_3CN of crystalliza-

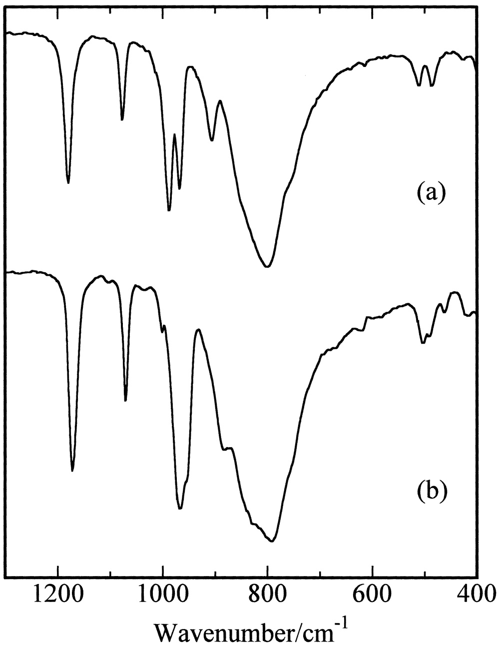

Fig. 1. IR spectra of (a) $(n\text{-}Pr_4N)_4[S_2W_{18}O_{62}]$ and (b) $(n\text{-}Pr_4N)_4[S_2Mo_{18}O_{62}]$ in the KBr pellets. Numerical data are given in the text.

tion was detected. For the $n\text{-}Pr_4N^+$ salt dissolved in CH_3CN, a major Raman line was obtained at 1007 cm^{-1}. IR (KBr) 1180, 1076, 986, 966, 906, 804, 512, 486 cm^{-1} (Fig. 1a). For comparative studies, the $n\text{-}Pr_4N^+$ salt of the α-Dawson-type $(n\text{-}Pr_4N)_4[S_2Mo_{18}O_{62}]$ complex was prepared according to our previous procedures.[10] IR (KBr) 1170, 1070, 966, 880, 792, 504, 490, 462 cm^{-1} (Fig. 1b).

Structure Determination. Single crystals were obtained by slow evaporation of a CH_3CN solution of the $n\text{-}Pr_4N^+$ salt at room temperature, being subjected to a single-crystal X-ray diffraction analysis. The crystal was mounted on a glass capillary and covered with epoxy resin. The intensity data were collected on a Rigaku RAXIS-RAPID Imaging Plate diffractometer with graphite-monochromated Mo $K\alpha$ radiation ($\lambda = 0.71069$ Å) at ambient temperature (298 ± 2 K). Lorenz poralization and numerous absorption corrections were applied using the TEXSAN program package.[14] All calculations were carried out with the SHELX97[15] program at the Computer Center, Institute for Molecular Science. Experimental details and crystallographic data are summarized in Table 1. The 18 W atoms were located by a direct method, and all other non-H atoms were found by successive difference Fourier syntheses. The W and S atoms were refined anisotropically, and the O and N atoms were refined isotropically. Refinement of the positions of carbon atoms in the $n\text{-}Pr_4N$ cations led to a divergence of the positional parameters, probably due to their large thermal motion. Therefore, positions of all C atoms were fixed at those from the Fourier map, and the thermal parameters were refined isotropically. For the solvent of crystallization, CH_3CN, both the positional and thermal parameters were fixed for the same reason. The enantiomer was checked as "racemic twinning" in the calculations. The results of the refinements are also summarized in Table 1.

Table 1. Experimental Details, Crystallographic Data and Results of Refinements for $[(n\text{-}C_3H_7)_4N]_4[S_2W_{18}O_{62}]\cdot CH_3CN$

Formula	$C_{50}H_{115}N_5O_{62}S_2W_{18}$
FW	5151.89
Crystal	orthorhombic
Space Group	$Pca2_1$(No. 29)
a/Å	27.181(1)
b/Å	14.1428(6)
c/Å	27.7292(9)
V/Å^3	10659(1)
D_{calc}/Mg m^{-3}	3.20
Z	4
F(000)	9240
μ(Mo $K\alpha$)/mm^{-1}	19.39
Color of crystal	pale yellow
Crystal dimensions/mm^3	0.35 × 0.10 × 0.07
No. refln. and 2θ range used for cell determination	52589(4.2 − 41.6°)
Data Images	74 exposures at 0.2 min per degree
Oscillation range ($\phi = 0.0°$, $\chi = 45.0°$)	ω 130.0–190.0° with 3.0° step
($\phi = 180.0°$, $\chi = 45.0°$)	ω 0.0–162.0° with 3.0° step
Camera radius	127.40 mm
2θ max measd.	55.0°
No. refln. measd.	40623
No. refln. unique	12133
No. refln. used	12095
No. parameters	500
Transmission factors	0.0835–0.3907
Refinement	full matrix on F^2
$R1$ and $wR2$ for $F^2 > 2.0\sigma(F^2)$*	0.0437, 0.0962
Goodness of Fit on F^2	0.841
Largest peak and hall/e Å^{-3}	2.46, −3.08

*Weighting scheme: $w = 1/[\sigma^2(F_o^2) + (0.64P)^2]$, $P = [0.33333(0, F_o^2)_{max} + 0.66667F_c^2]$

Crystallographic data have been deposited at the CCDC, 12 Union Road, Cambridge CB2 1EZ, UK and copies can be obtained on request, free of charge, by quoting the publication citation and the deposition numbers CCDC-164731. The data are also deposited at Document No. 74047 at the Office of the Editor of Bull. Chem. Soc. Jpn.

Results and Discussion

Crystallographic Studies. Refinements of the atomic parameters gave no unreasonable results for those in the polyanion. However, the accuracy of the positional parameters is not good enough (four digits even for y and z of tungsten atoms). This is probably caused by a rather poor quality of the crystal, which caused an inaccurate determination of the $n\text{-}Pr_4N^+$ cations and CH_3CN, and rather strong correlations of the parameters in the structure refinement.

An ORTEP[16] view along with atomic notations and a polyhedral model of the polyanion are shown in Fig. 2. The polyanion has the normal feature of the so-called α-Dawson structure with a formula of $[S_2W_{18}O_{62}]^{4-}$. A pair of so-called A-type 3-lacunary α-Keggin nonatungstosulfate units,

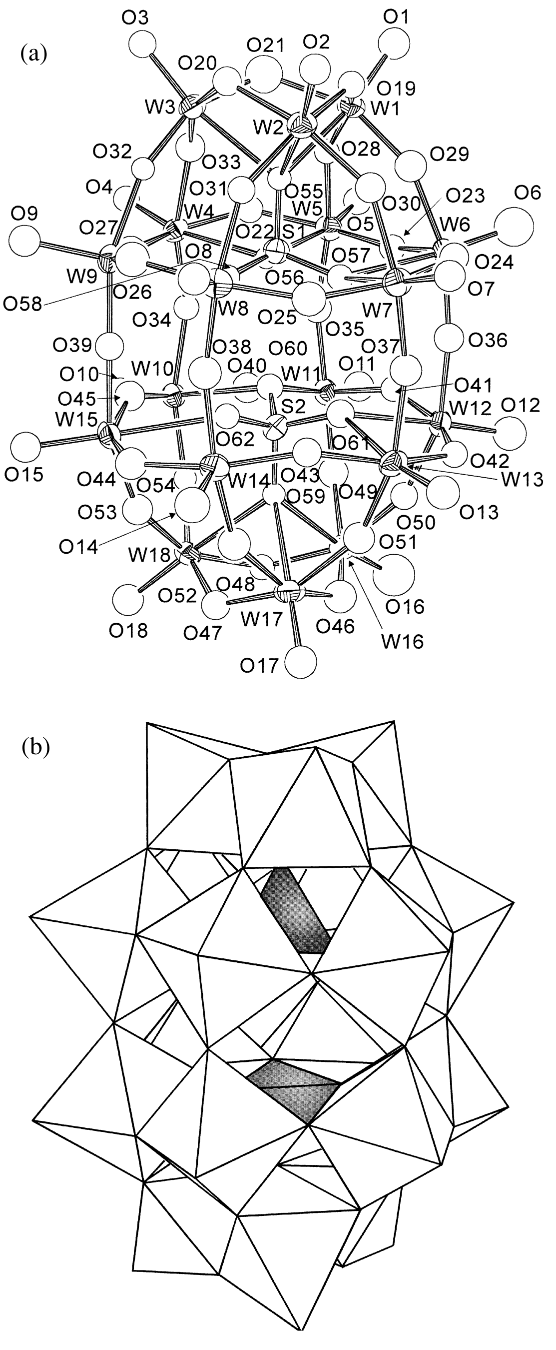

Fig. 2. An ORTEP view along with atomic notations (a) and a polyhedral representation (b) of the α-$[S_2W_{18}O_{62}]^{4-}$ anion.

$[SW_9O_{34}]^{8-}$, formed by removing three adjacent corner-sharing WO_6 groups from the α-Keggin structure, are linked by sharing six oxygen atoms, which stick out to the "lacunary" positions. It is isostructural to the Mo-analogue $[S_2Mo_{18}O_{62}]^{4-}$.[10] However, the torsion of the "top" and "bottom" M_3-triangles is smaller in this W-complex than in the Mo-analogue. The selected interatomic distances are listed in Table 2. No unacceptable distance or angle in the polyanion was observed, except for some rather long W–O (terminal) distances. The accuracy of the distances and angles are, however, again not good enough. The reason is most probably due to the poor quality of the crystal, as mentioned above. Each of the two SO_4-units shows a slightly distorted tetrahedron. The S–O distances range from 1.42(3) to 1.54(3) Å for S1 and 1.48(3) to 1.54(3) Å for S2. The valence[17] of each S atom was calculated as 5.83 for S1 and 5.53 for S2; the mean value is 5.68, which is acceptable. Each W atom is surrounded by six oxygen atoms, one terminal and five bridging to W or S atom, to form an octahedron. The W atom is displaced slightly from the center of the octahedron towards the direction of the terminal O atom. The W–O bonds can be assorted into four groups: W–O (terminal) 1.65(3) to 1.82(3) Å, W–O (bridging W–O–W in the W_6O_{13} or W_2O_{10} unit) 1.85(3) to 2.03(3) Å, W–O (bridging W–O–W between W_6O_{13} or W_2O_{10} units) 1.80(3) to 2.05(3) Å, and W–O (bridging W–O–S) 2.39(3) to 2.57(3) Å. These values are in a similar range with those of the Mo-analogue, and are quite normal for a compound of this type. The averaged bond valence[17] of W is 6.06, which agrees with the expected value of 6.0, although the calculated values range from 5.35 to 6.65, probably due to some uncertainty in the positions of the oxygen atoms.

Voltammetric Characterization of $[S_2W_{18}O_{62}]^{4-}$. Figure 3 shows cyclic voltammograms of 0.50 mM $[S_2W_{18}O_{62}]^{4-}$ in CH_3CN containing 0.1 M n-Bu_4NClO_4. In the absence of H^+, $[S_2W_{18}O_{62}]^{4-}$ exhibited a four-step one-electron redox wave with mid-point potentials (E_{mid}) of -0.18, -0.56, -1.12, and -1.51 V, where $E_{mid} = (E_{pa} + E_{pc})/2$; E_{pc} and E_{pa} are cathodic and anodic peak-potentials, respectively. The separation of the E_{pc} and E_{pa} values for each redox couple, ΔE, averaged (62 ± 3) mV, indicating the reversible nature of each wave. For the sake of brevity, the one-electron waves were expressed as A, B, C, and D.

With the addition of CF_3SO_3H, a new wave, denoted as B′, appeared and grew at potentials more positive than wave B. This behavior is accounted for in terms of protonation of the two-electron reduced species at the electrode surface.[17–23] Wave B′ was succeeded by waves C′ and D′. Wave D′ occurred at the same potential as wave C. As a result, waves B, C, and D disappeared completely. It should be noted that the first one-electron reduction proceeded without the consumption of protons, because the wave shape and peak position of wave A were unchanged.

As the CF_3SO_3H concentration was increased, waves E and F grew and became two-electron waves. At CF_3SO_3H concentrations greater than 3 mM, wave B′ moved closer to wave A, which still remained unchanged. Ultimately, they merged into a two-electron wave in the presence of 10 mM CF_3SO_3H, giving three two-electron redox waves with E_{mid} values of -0.15, -0.36, and -0.61 V (Fig. 3d).

With the addition of 1% (v/v) water, as shown in Fig. 3e, the first two-electron wave was split into two one-electron waves with E_{mid} values of -0.17 and -0.35 V, giving rise to one-, one-, two-, and two-electron waves. A similar transformation of a two-electron wave into two one-electron waves was also observed for α- and β-Keggin-type $[PW_{12}O_{40}]^{3-}$ complexes in CH_3CN.[21] With the addition of water, the acidity strength decreased due to the formation of oxonium ions, because protons are only weakly bonded to CH_3CN.[24]

Formation of $[S_2W_{18}O_{62}]^{4-}$ in Aqueous-CH_3CN Media. Raman Spectroscopy. In order to clarify the formation con-

Table 2. Selected Interatomic Distances/Å in the Polyanion $[S_2W_{18}O_{62}]^{4-}$

Atom	Distance	Atom	Distance	Atom	Distance	Atom	Distance
W1–O1	1.76(4)	W6–O6	1.66(5)	W11–O11	1.74(3)	W16–O16	1.82(5)
–O19	1.96(2)	–O23	1.94(2)	–O35	1.92(3)	–O46	1.90(3)
–O21	1.99(4)	–O24	1.92(3)	–O40	1.85(3)	–O48	1.87(3)
–O28	1.86(2)	–O29	1.98(3)	–O41	1.92(3)	–O49	1.96(3)
–O29	1.83(3)	–O36	1.84(3)	–O49	1.84(3)	–O50	1.95(3)
–O55	2.39(3)	–O57	2.51(3)	–O60	2.41(3)	–O59	2.52(2)
W2–O2	1.76(3)	W7–O7	1.70(3)	W12–O12	1.72(4)	W17–O17	1.69(3)
–O19	1.86(3)	–O24	1.86(3)	–O36	1.93(3)	–O46	1.88(3)
–O20	1.94(3)	–O25	1.93(4)	–O41	1.92(2)	–O47	1.90(3)
–O30	1.87(3)	–O30	1.98(3)	–O42	1.90(2)	–O51	1.97(3)
–O31	1.90(3)	–O37	1.85(3)	–O50	1.83(3)	–O52	2.00(3)
–O55	2.51(2)	–O57	2.49(2)	–O61	2.47(3)	–O59	2.54(2)
W3–O3	1.71(3)	W8–O8	1.70(3)	W13–O13	1.65(3)	W18–O18	1.81(3)
–O20	1.94(2)	–O25	1.86(3)	–O37	1.93(3)	–O47	1.95(3)
–O21	1.90(4)	–O26	1.90(3)	–O42	1.93(3)	–O48	1.90(3)
–O32	1.83(3)	–O31	1.93(3)	–O43	1.95(3)	–O53	1.99(3)
–O33	1.87(3)	–O38	1.83(3)	–O51	1.83(3)	–O54	1.93(3)
–O55	2.39(3)	–O58	2.47(2)	–O61	2.48(3)	–O59	2.51(2)
W4–O4	1.75(3)	W9–O9	1.80(3)	W14–O14	1.76(3)	S1–O55	1.54(3)
–O22	1.99(3)	–O26	1.98(3)	–O38	1.96(3)	–O56	1.51(2)
–O27	1.80(3)	–O27	1.99(3)	–O43	1.88(3)	–O57	1.48(3)
–O33	2.05(3)	–O32	2.00(3)	–O44	1.88(3)	–O58	1.42(3)
–O34	1.81(3)	–O39	1.82(3)	–O52	1.84(3)	S2–O59	1.49(3)
–O56	2.43(2)	–O58	2.48(3)	–O62	2.47(3)	–O60	1.54(3)
W5–O5	1.67(3)	W10–O10	1.77(3)	W15–O15	1.77(3)	–O61	1.51(3)
–O22	1.86(3)	–O34	2.00(3)	–O39	1.98(3)	–O62	1.48(3)
–O23	1.83(3)	–O40	2.03(4)	–O44	1.97(3)		
–O28	1.99(2)	–O45	1.88(3)	–O45	1.95(3)		
–O35	1.87(3)	–O54	1.88(3)	–O53	1.84(3)		
–O56	2.45(2)	–O60	2.57(3)	–O62	2.54(3)		

ditions of $[S_2W_{18}O_{62}]^{4-}$, Raman spectra were recorded for a 50 mM W(VI)–2 M H_2SO_4–40%(v/v) CH_3CN system, and are shown in Fig. 4. When measurements were made without heating, a pair of lines was observed at 1003 and 989 cm^{-1}. We have recently demonstrated that $[W_6O_{19}]^{2-}$, which does not exist in any appreciable amounts in aqueous solution, is markedly stabilized by the presence of CH_3CN; the 1003 cm^{-1} line is assigned to $[W_6O_{19}]^{2-}$, and the 989 cm^{-1} line to $[W_{10}O_{32}]^{4-}$.[25] The big Raman lines at 1054 and 924 cm^{-1} are assigned to the absorption of HSO_4^- and CH_3CN, respectively. After heating the solution at 70 °C, it turned to yellow, and the 1003 cm^{-1} line increased along with a slight shift to greater wavenumbers, eventually to 1007 cm^{-1}. Simultaneously, the 989 cm^{-1} line gradually decreased along with a change in the peak shape; at present, this behavior cannot be accounted for. On the basis of the fact that the Raman frequency of $[S_2W_{18}O_{62}]^{4-}$ is obtained at 1007 cm^{-1} in CH_3CN, the 1007 cm^{-1} line can be assigned to the α-Dawson complex. This is further supported by the fact that the Raman intensity due to $[W_6O_{19}]^{2-}$ at 1003 cm^{-1} is practically unaffected by heating of the W(VI)–HCl–CH_3CN system. The Raman line assigned to $[S_2W_{18}O_{62}]^{4-}$ was obtained in the H_2SO_4 concentration range of 1.0–3.5 M. The $[S_2W_{18}O_{62}]^{4-}$ complex was stable under these conditions, as judged from the fact that the Raman intensity did not change with time.

Electrochemistry. In order to complement the Raman results, cyclic voltammograms were recorded for a 50 mM W(VI)–2 M H_2SO_4–40%(v/v) CH_3CN system. When a voltammogram was recorded for a freshly prepared solution, as shown in Fig. 5a, a redox wave due to $[W_{10}O_{32}]^{4-}$ was obtained with an $E_{\rm mid}$ value of -0.12 V, followed by an ill-defined wave.[25] When the cyclic voltammogram was recorded again after heating the solution for 6 h at 70 °C, new waves appeared at more positive potentials, along with a decrease in the reduction wave of $[W_{10}O_{32}]^{4-}$. After 24-h of heating at 70 °C, a four-step redox wave with a current ratio of 1 : 1 : 2 : 2 was obtained with $E_{\rm mid}$ values of 0.21, -0.02, -0.28, and -0.50 V (Fig. 5c). From the results in Fig. 3e and Fig. 4c, it follows that the four-step wave can be ascribed to the reduction of $[S_2W_{18}O_{62}]^{4-}$. The four-step wave was obtained in the H_2SO_4 concentration range of 1.0–3.5 M, in agreement with the Raman results.

The presence of CH_3CN was essential for the formation of $[S_2W_{18}O_{62}]^{4-}$ at concentrations $> 20\%$ (v/v); however, a solution of two liquid layers resulted at CH_3CN concentrations of 50% (v/v) or more. The $[S_2W_{18}O_{62}]^{4-}$ complex was not formed at any appreciable concentrations in the presence of other water-miscible organic solvents, such as ethanol, acetone, 1,4-dioxane, *N*-methylformamide, dimethyl sulfoxide, and propylene carbonate.

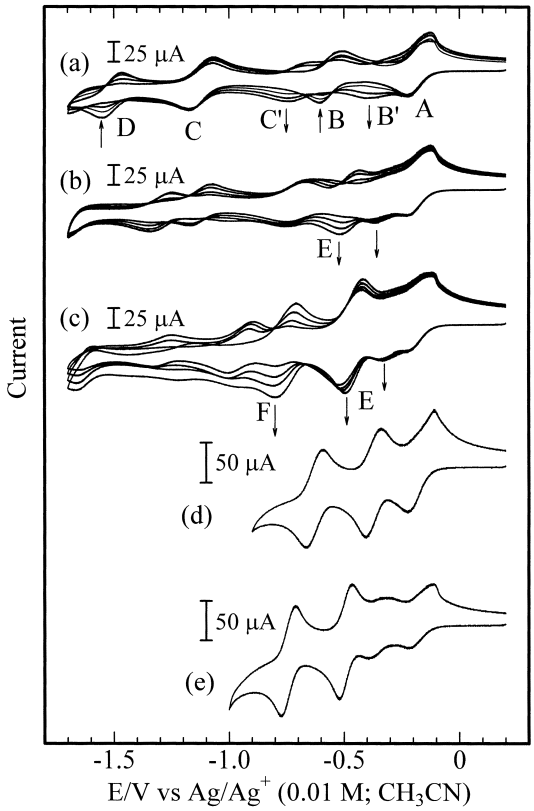

Fig. 3. Cyclic voltammograms of 0.50 mM $[S_2W_{18}O_{62}]^{4-}$ in CH$_3$CN containing 0.1 M n-Bu$_4$NClO$_4$. [CF$_3$SO$_3$H]/mM: (a) 0–0.3; (b) 0.4–0.7; (c) 1.2–2.0; (d) 10; (e) (d) with 1% (v/v) H_2O.

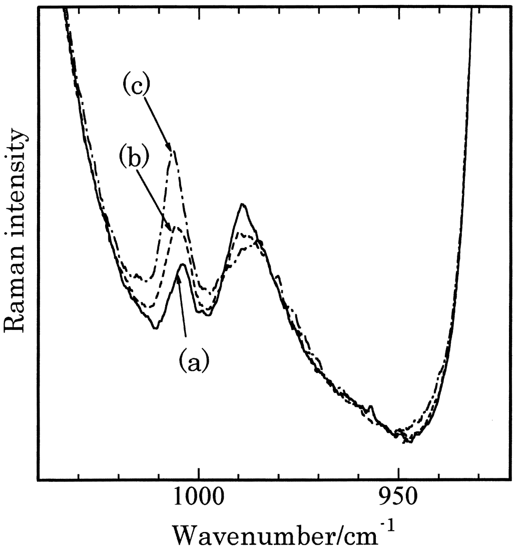

Fig. 4. Raman spectra for a 50 mM W(VI)–2 M H_2SO_4–40% (v/v) CH$_3$CN system. Recorded (a) without heating; after heating 70 °C for (b) 6 and (c) 24 h.

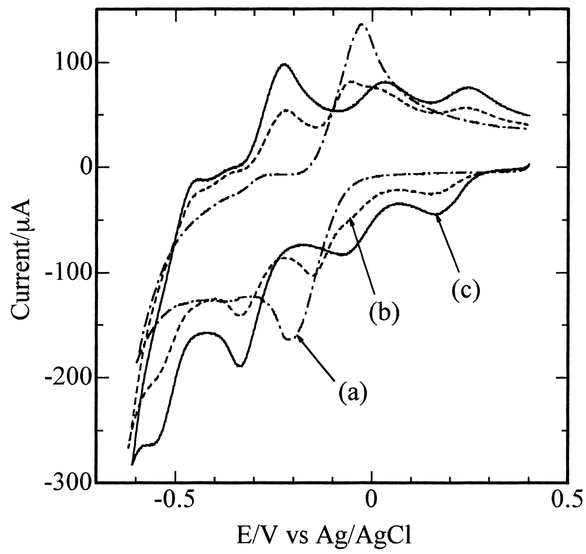

Fig. 5. Cyclic voltammograms for a 50 mM W(VI)–2 M H_2SO_4–40%(v/v) CH$_3$CN system. Measured (a) without heating; after heating 70 °C for (b) 6 and (c) 24 h.

References

1 B. Dawson, *Acta Crystallogr.*, **6**, 113 (1953).

2 H. D'Amour, *Acta Cryst.*, **B32**, 729 (1976).

3 R. Acerete, S. P. Harmalker, C. F. Hammer, M. T. Pope, and L. C. W. Baker, *J. Chem. Soc., Chem. Commun.*, **1979**, 777.

4 R. Massart, R. Contant, J. M. Fruchart, J. P. Ciabrini, and M. Fournier, *Inorg. Chem.*, **16**, 2916 (1977).

5 K. Matsumoto and Y. Sasaki, *J. Chem. Soc., Chem. Commun.*, **1975**, 691.

6 R. Contant and R. Thouvenot, *Can. J. Chem.*, **69**, 1498 (1991).

7 R. Strandberg, *Acta Chem. Scand.*, **A29**, 350 (1975).

8 H. D'Amour and R. Allmann, *Naturwiss.*, **61**, 34 (1974).

9 S. Himeno, M. Hashimoto, and T. Ueda, *Inorg. Chim. Acta*, **284**, 237 (1999).

10 a) T. Hori and S. Himeno, *Chem. Lett.*, **1987**, 53. b) S. Himeno, T. Hori, and A. Saito, *Bull. Chem. Soc. Jpn.*, **62**, 2184 (1989). c) T. Hori, O. Tamada, and S. Himeno, *J. Chem. Soc., Dalton Trans.*, **1989**, 1491.

11 a) S. Himeno, T. Hori, H. Tanaka, and A. Saito, *Chem. Lett.*, **1988**, 343. b) T. Hori, S. Himeno, and O. Tamada, *J. Chem. Soc., Dalton Trans.*, **1992**, 275.

12 a) S. Himeno, K. Miyashita, A. Saito, and T. Hori, *Chem. Lett.*, **1990**, 799. b) T. Hori, S. Himeno, and O. Tamada, *J. Chem. Soc., Dalton Trans.*, **1996**, 2083.

13 P. J. S. Richardt, R. W. Gable, A. M. Bond, and A. G. Wedd, *Inorg. Chem.*, **40**, 703 (2001).

14 Molecular Structure Corporation, TEXSAN: Crystal Structure Analysis Package, Research Forest Drive, The Woodlands, Texas, USA (1985, 1999).

15 G. M. Sheldrick, SHELX97, University of Göttingen, Germany (1997).

16 Johnson C. K., ORTEPII. Report ORNL-5138, Oak Ridge National Laboratory, Tennessee, USA (1976).

17 N. E. Brese and M. O'Keefe, *Acta Crystallogr., Sect. B*, **47**, 192 (1991).

18 S. Himeno, T. Osakai, A. Saito, K. Maeda, and T. Hori, *J. Electroanal. Chem.*, **337**, 371 (1992).

19 K. Maeda, S. Himeno, T. Osakai, A. Saito, and T. Hori, *J. Electroanal. Chem.*, **364**, 149 (1994).

20 S. Himeno, K. Maeda, T. Osakai, A. Saito, and T. Hori,

Bull. Chem. Soc. Jpn., **66**, 109 (1993).

21 S. Himeno, M. Takamoto, and T. Ueda, *J. Electroanal. Chem.*, **465**, 129 (1999).

22 S. Himeno, M. Takamoto, and T. Ueda, *J. Electroanal. Chem.*, **485**, 49 (2000).

23 M. Sadakane and E. Steckhan, *Chem. Rev.*, **98**, 219 (1998).

24 S. Himeno and A. Saito, *J. Electroanal. Chem.*, **391**, 207 (1995).

25 S. Himeno, M. Yoshihara, and M. Maekawa, *Inorg. Chim. Acta*, **298**, 165 (2000).